Multi-response optimization of bamboo/PALF–TiC hybrid composites for enhanced mechanical and tribological performance

R Saravanan[1*], *K* Loganathan[2], *S* Manoj Kumar[3], *Kaviarasan* Varadaraju[4], *K* Yoghananthan[5], and *Rojalin* mishra[6]

[1]Department of Robotics and Automation, Rajalakshmi Engineering College, Chennai, Tamil Nadu, India
[2]Department of Mechanical Engineering, Rajalakshmi Engineering College, Chennai, Tamil Nadu, India
[3]Department of Mechanical Engineering, Madanapalle Institute of Technology and Science, Madanapalle, Andhra Pradesh, India
[4]Department of Mechanical Engineering, Sona college of Technology, Salem, Tamil Nadu, India
[5]Department of Chemistry, Kongu Engineering College, Perundurai, Tamil Nadu, India
[6]Department of Electronics and Telecommunication, Gandhi Institute of Excellent Technocrat, Bhubaneswar, Odisha, India

Abstract. Researchers have developed alternative materials which incorporate diverse fillers and reinforcements in response to increasing requirement wear-resistant hybrid substances. Recent research had shown that hybrid composites made from a mix of natural fibers then ceramic fillers can improve tribological properties of materials used in automobiles and airplanes. A composite with improved tribological and mechanical characteristics at low cost can be achieved by combining natural fibers with ceramics using appropriate multi-response optimization approaches, despite the fact that natural fibers have certain drawbacks. This research delves into the wear behavior of a hybrid composite made of bamboo and PALF, filled with titanium carbide (TiC). Furthermore, this study employs a multi-response optimization method that integrates MOORA with the fuzzy model interference system. To find the lowest possible wear rate and coefficient of friction (COF), the Taguchi L27 orthogonal array (OA) was used in the experimental design. The investigation found that, the best working settings were 1 wt% TiC, 30 wt% reinforcement, 1.5 m/s sliding speed, 15 N load and 1500 m sliding distance with an Entropy - MOORA value of 0.804 and a MOORA fuzzy analysis (MFA) value of 0.801. The worn-out surface mechanisms, and tiny debris were all shown by scanning electron microscopy (SEM) to play a substantial role at achieving appropriate wear properties. In addition, mechanical properties were investigated in both wet and dry environments to determine optimal combination of particle hybrid composite.

* Corresponding author : saravanan.r@rajalakshmi.edu.in

1 Introduction

Innovative tribo-based materials have recently been sought after by the aerospace and automotive industries as a replacement for conventional synthetic materials used in extreme service and harsh environments. A polyester-based biocomposites reinforced with bamboo fiber and cassava biomass-derived biosilica was developed. The composite with 40 vol.% fiber and 5 vol.% biosilica showed the best mechanical, thermal, wear, and water-resistance properties, suitable for industrial and structural applications [1]. Hybrid composites using silane-treated bamboo and basalt fibers with sea urchin-derived chitin were fabricated. At 4% chitin, mechanical strength was maximized, while 8% chitin improved wear resistance, flame retardancy, and hydrophobicity [2]. Ramie and PALF fiber-reinforced epoxy hybrid composites were fabricated by hot press moulding and optimized using the Taguchi method. The best properties were achieved at 20 mm fiber length and 30 wt.%, with tensile (36.54 MPa), flexural (48.18 MPa), and impact strength (4.5 J), along with improved absorption and crystallinity [3]. PALF/epoxy composites reinforced with SiO_2 nanoparticles (3–9 wt%) were produced. Optimal performance occurred at 25% PALF and 6% SiO_2, showing improved mechanical, thermal, and water uptake properties, making them suitable for construction, packaging, and automotive applications [4]. Epoxy composites reinforced with NaOH-treated PALF and nanoclay were fabricated. The combination of 30 wt% PALF with 1.5 wt% nanoclay yielded the best tensile and flexural strength, while higher nanoclay (3 wt%) led to agglomeration and reduced properties [5]. Bio-epoxy composites reinforced with sisal/hemp fibers, Kevlar, and fillers (fly ash, TiC) were tested before and after 5 months of accelerated weathering. Results showed reduced mechanical and thermal performance post-weathering, though fillers improved resistance against UV and moisture degradation [6]. Recycled polystyrene composites reinforced with 10–20 wt% sugarcane bagasse cellulose fibers were produced and tested. The addition of lignin-rich fibers improved stiffness and heat deflection temperature, while overall thermal stability decreased slightly, confirming EPS composites as a viable recycling route [7]. A multi-stage bamboo fiber treatment (ozone–enzyme–H_2O_2) reduced gum and lignin by over 70%, improving fiber fineness, cleanliness, and tensile strength (4.58 cN/dtex). This eco-friendly synergistic method enhances fiber quality for biomedical textiles, bio-composites, and absorbent applications [8]. A bonding interface design using dual molecular weight resin impregnation improved bamboo fiber composites. The optimized BFRC achieved higher strength (MOR 197 MPa, compressive 142 MPa) and better water resistance, supporting applications in shipbuilding and extreme environments [9]. Long bamboo fibers prepared by peroxyformic acid-assisted roller pressing showed high cellulose retention and tensile strength (658.58 MPa). Epoxy resin impregnation improved durability and alkali resistance, making them promising reinforcements for cement-based composites [10]. The literature study makes it quite evident that when dealing with composite materials' multi-response tribological behavior, it is critical to identify and optimize the important process parameters. A balanced and methodical approach is necessary since optimizing performance parameter can have unintended consequences on other parameters. This paper employs a Gray Relational Analysis (GRA) approach based on integrated fuzzy logic to find the most effective and secure operational settings. This approach considers the inherent uncertainty and unpredictability of experimental data. Building a robust and comprehensive multi-response optimization model is the unique contribution of this work. The model ensures enhanced operating safety and dependability in harsh conditions and also provides precise prediction and optimization in cases of complicated, nonlinear interactions. Furthermore, the proposed approach successfully reduces the amount of time and money spent on experiments while keeping the difference between the anticipated and experimental values to a minimum, demonstrating its usefulness in the real world and in industry.

2 Materials and methodology

2.1 Materials used

A PALF woven mat and a bamboo woven mat are the reinforcing materials for this work. The matrix material was made of high-quality epoxy resin, specifically Araldite LY556. A mixture of 10:1 epoxy resin and anhydride hardener (HY951 grade) was used. To achieve a uniform dispersion of TiC, acetone and dimethylformamide (DMF) was used. PALF and bamboo fiber, noted for their high thermal stability, exceptional mechanical strength and long-lasting qualities were used as reinforcement materials. The filler material, TiC (15 μm) powder was sourced from Matrix enterprises, Nagercoil, Tamilnadu, India. and is renowned for its durability, high melting point and chemical stability. The chemical name of the epoxy resin utilized in this study is Bisphenol-A-diglycidyl-ether and it is grade LY556. The substance is transparent and has a pale-yellow color. At 25 °C, its density is 1.1-1.2 g/cm³ and its viscosity ranges from 10,000 to 12,000 MPa·s. Grade HY951 also known as 2-amineethylethane-1,2-diamin is used as a hardener. It is transparent and has a specific gravity of 0.98 g/cm³ at 20 °C. Natural reinforcements included bamboo fiber (in the form of a non-woven mat) and pineapple leaf fiber (PALF), both of which had densities of about 1.30 g/cm³ and 1.46 g/cm³, respectively. The particulate filler was titanium carbide (TiC) powder, which had a surface area of 200 m²/g and a density of around 4.9 g/cm³.

2.2 Design of experiments (DoE) framework

To determine how different independent variables affected the dependent variables, the Taguchi design of experiments was used. Table 1 displays the five-level organizational structure of the present study, which includes the following factors: filler weight, reinforcement weight, sliding distance, normal load and sliding speed. Each factor has 3 levels. The experiments were carried out three times using a Pin-on-disk apparatus with a 30 mm × 10 mm specimen size as per ASTM G99.

Table 1. Aspects and degrees of the experiment.

Parameters	Notations	Units	Levels		
			1	2	3
Gr/TiC	A	wt.%	1.5	2.5	3.5
Reinforcement	B	wt.%	15	25	35
Sliding distance	C	m	450	900	1350
Sliding speed	D	m/s	0.6	1.2	1.8
Load	E	N	6	12	18

According to research, increasing the amount of nano filler in a material can cause particles to clump together in the polymer matrix, which can cause a suspension if there is even more nano filler. TiC fillers were included at weights of 1.5, 2.5, and 3.5%. With a filler concentration of 15-35%, lubrication's C-C bond then high Van der Waals forces decreased friction by 36% and wear by 32%. In addition, when the TiC filler percentage went over 3.5 wt%, the hybrid composite's mechanical and tribological characteristics started to decline because the filler particles tended to clump together. Furthermore, reinforcing was provided with bamboo/PALF fibers (15, 25, 35% by weight). More than 35% reinforcement experiences an increase in micro voids, fiber clustering, porosity, and fracture propagation as a result of uncontrolled variables.

There was an issue with the thermal stress distribution across the interface after 1800 m of sliding distance due to the composite's lower frictional performance caused by hard-to-hard contact and disk rotation with counter surface. Therefore, sliding distance levels of 450 m, 900 m, and 1350 m were selected. Friction increased, acute wear loss was significant, and wear debris was distributed throughout the worn surface as a result of increased plastic deformation and delamination. Prior authors have demonstrated that different sliding speeds affect wear rate. Because of the increased acute contact area and superior contact temperature at the counter interface, the soft matrix might melt there. This reduces the matrix shear strength, increases fiber pullout, and, at high sliding speeds, generates furrows on the surface of the fibers. Thus, when fibers come into contact with steel counter surfaces, they create a more uniform tribofilm with a smoother distribution and better adhesion to the counterpart. This leads to the development of sufficient wear debris, which in turn reduces wear and the coefficient of friction. It is clear that increased surface temperature and wear can occur under higher loads. Consequently, the wear rate can increase by approximately 197.7% and the coefficient of friction by about 93.9%.

2.3 Fabrication of composite laminate

One step in making these fibers is pre-treating them with 5% NaOH by weight. This will make the matrix adhere better. Using the solution casting technique, a hybrid composite with TiC included at three distinct concentrations was created. By using a probe sonicator set at 70˚C for 30 minutes, DMF and acetone are introduced into TiC. To ensure that the acetone evaporates entirely, the TiC solvent combination is mixed with the appropriate amount of epoxy solution and then swirled in magnetic stirrer at 60˚C for 30 minutes at 300 rpm. In a bath ultrasonicator set at 70˚C for 30 minutes, ultrasonic waves are utilized to create a uniform combination of epoxy and TiC. To create a consistent ceramic hybrid material, the fibers were sized correctly and combined with an epoxy resin mixture. The mixture was then compressed in a compression molding for around 45 minutes at 120 °C with a constant pressure of 10 MPa to provide sufficient compaction. Prior to post-curing, the pressure was kept at 6 MPa for about 5 minutes so as not to harm the laminate. Samples can be more easily removed from molds with the use of titanium spray. The next step is to post-cure it for another 24 hours at a temperature much higher than ambient (60 °C) in an open atmosphere. The hybrid composite with TiC filler was manufactured according to the steps shown in Figure 1. The created material was then bonded into 300 mm × 300 mm × 3 mm blocks.

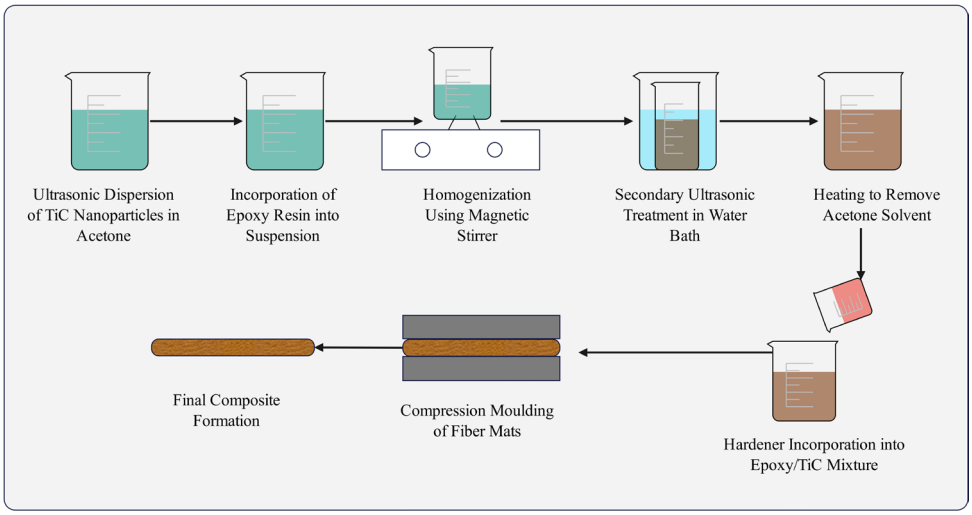

Fig. 1. Fabrication process of TiC-reinforced Bamboo/PALF hybrid composite.

2.4 Physico-mechanical characterization of hybrid composite

2.4.1 Wear and friction test

In accordance with ASTM G99-05, the experiments were conducted. In order to reduce the possibility of experimental error, the Taguchi orthogonal array was used to conduct two tests on each sample. Using Eq. 1 to determine the usual steady-state coefficient of friction, the analysis was conducted.

$$\mathrm{COF} = \frac{F}{W} \tag{1}$$

In this case, F is the frictional force and W is the load. The weight of the sample was measured both before and after the tribological test in order to determine the volume loss, as given in Eq. 2. After that, we use Eq. 3 to determine the SWR.

$$\mathrm{V_{loss}} = \frac{m_{\mathrm{loss}}}{\rho} \tag{2}$$

$$\mathrm{S} = \frac{V_{\mathrm{loss}}}{W \times L} \tag{3}$$

where the mass loss is denoted by m the volume loss is denoted by v-loss, and the bulk density is denoted by ρ/g. L is the sliding distance in meters, and S is the specific wear rate in mm/nm for Eq. 3.

2.4.2 Water absorption test

Following the guidelines laid out by ASTM D570-98, the water absorption tests were carried out. A sample of 20 × 20 × 10 mm was used. To start, we weighed the samples after they had dried in a hot air oven. After that, for 10 days at room temperature (32 °C), they were immersed in a water bath. Weight growth was calculated by subtracting the initial weight from the end weight, which was recorded every 24 hours along with the wet weight. After 10 days Eq. 4 was used to determine how much water each sample had absorbed. Equation 4 was used to calculate the water absorption for the samples.

$$\text{Water absorption } \% = \left[\frac{\text{Wet } - \text{Dry weight}}{\text{Dry weight}}\right] \times 100 \quad (4)$$

2.4.3 Mechanical test

Composites were subjected to a series of mechanical testing, including tensile, impact, flexural and hardness, in both dry and wet conditions. A Universal Testing Machine with a 100 KN cell was used to measure tensile strength in accordance with ASTM D638 requirements. A steady speed of 5 mm/min was used to conduct the test on rectangular specimens with dimensions of 200×25×4 mm. The results were averaged after each sample underwent three independent analyses. The definition of flexural strength in ASTM D790 was identical to the same UTM with a cross head speed of 5−mm/min was used. The dimensions of flexural sample were 150×25×4 mm. Like tensile testing, the three readings from each sample and averaged values were noted. The impact strength were measured by Izod Impact Tester, is defined by ASTM D256. The composites' ability to absorb energy was evaluated by impacting samples with dimensions of 60×12.5×3 mm. The samples was tested three times with average reading recorded each time. Shore D hardness defined as a material's resistance to localized plastic deformation caused by mechanical indentation, was determined using the Shore D Durometer and ASTM D2240 standards. A load of 49 N was applied for five seconds during the test. To calculate the theoretical hardness (H) of the composites by dividing the applied force by projected indentation surface area (Equation 5):

$$\text{H} = \frac{F}{S} \quad (5)$$

2.5 Ranking method

2.5.1 Attribute weight calculation

Objective weighting procedures do not require decision-makers to furnish previous knowledge or decision-making, unlike subjective methods. The methodology employed for determining attribute weights with the entropy method is outlined as follows:

$$D = \begin{bmatrix} x_{11} & x_{12} & x_{13} & x_{14} \\ x_{21} & x_{22} & x_{23} & x_{24} \\ x_{31} & x_{32} & x_{33} & x_{34} \end{bmatrix} \quad (6)$$

Equation (6) illustrates the decision matrix "D" pertaining to the current multi-criteria situation. In the entropy weighting approach, the decision matrix (Eq. (6)) is initially normalized for each attribute to derive the projection value (N_{ij}) using the subsequent formula;

$$N_{ij} = \frac{x_{ij}}{\sum_{i=1}^{m} x_{ij}} \quad (7)$$

The entropy measure (e_j) for each property is subsequently calculated as follows;

$$e_j = -\kappa \sum_{j=1}^{n} N_{ij} \ln\left(N_{ij}\right) \quad (8)$$

Where, κ is a constant and defined as $\kappa = \frac{1}{\ln(m)}$

The variance of the information pertaining to the measurement of each attribute is calculated as;

$$D_j = 1 - e_j \quad (9)$$

The objective weight (ω_j) of each attribute is calculated using the entropy approach as follows:

$$\varpi_j = \frac{\partial_j}{\sum_{j=1}^{n} \partial_j} \tag{10}$$

Where, $\partial_j = 1 - e_j$ and subjected to; $\sum_{j=1}^{n} \omega_j = 1; \omega_j \geq 0$.

2.5.2 MOORA: ratio system approach

If a fixed number of options and to choose the best one out of them, the MOORA - MCDM approach is used. Although it advocates for the ratio system approach and utilizes fewer computations overall, the MOORA method is more resilient and can concurrently resolve many criteria. It also provides material alternatives with realistically correct ranks. Finally, we compare and contrast the ranks that each method produces. The first step of this method is to create a decision matrix that ranks all of the options according to a number of criteria. Summarizing the steps of the MOORA ratio scheme as follows:

Step 1: The i-th indicators that rank the choices according to the j_{th} criteria are arranged to produce the decision matrix X.

$$X = \left[x_{ij}\right]_{m \times n}. \tag{11}$$

Step 2: Equation 16 can be used to normalize a decision matrix.

$$\hat{x}_{ij} = \frac{x_{ij}}{\sqrt{\sum_{j=1}^{n} x_{ij}^2}}. \tag{12}$$

Step 3: Equation 11 provides one approach to constructing a normalized, weighted decision matrix. The value of w_j can be used to infer the weight given to the j_{th} criterion in this case. It is possible to estimate these weights using either the entropy method or the AHP technique. In this work, the AHP approach is used to estimate the weights.

$$V_i = \mathrm{W}_j x \hat{X}_{ij} \tag{13}$$

Step 4: Equation 14 is used to determine the final preference (y) values, where j = 1…g represents the criteria to maximize and j = g+1…n represents the criteria to minimize.

$$\tilde{y}_i = \sum_{j=1}^{g} v_{ij} - \sum_{j=g+1}^{g} v_{ij}. \tag{14}$$

Step 5: In order to find the ranking of the alternatives, the ~yi values are sorted from highest to lowest.

2.6 Fuzzy logic approach (FL)

When dealing with issues involving ambiguity, uncertainty or imprecision, the computational framework of fuzzy logic is ideal. Important in practical Engineering applications, fuzzy logic's capacity to deal with hard-to-model situations is a major advantage. The Mamdani fuzzy method were used in this study because it has many benefits. It can handle imprecision and uncertainty, makes better decisions, can model nonlinear and complex systems then incorporate expertise and human knowledge into decision-making process. Since this complicated parametric model produces uncertain and imprecise data, fuzzy logic is essential for evaluating it.

However, AI techniques based on fuzzy logic, including genetic algorithms and neural networks can fix this issue and provide more efficient and robust models. The following are the four stages involved in predicting the output responses:

- Humans establish the system's rules and circumstances in its rule base, sometimes called its knowledge base.
- Module for fuzzification: Fuzzification converts numerical numbers, which are crisp inputs into sets of fuzzy values. Crisp inputs are independent variables that are known for being accurate.
- The inference engine measures the degree to which fuzzy inputs conform to each rule. The control actions are created by combining these rules and deciding which ones to fire.
- This module is responsible for defuzzifying the data so that the inference engine can produce more precise results from fuzzy sets.

An FIS is used to create a fuzzy interface by connecting the fuzzifier and defuzzifier. Figure 2 shows the overall approach of MOORA-fuzzy logic. The fuzzification module sends fuzzy inputs to FIS, which processes them using a rule base editor. Decisions are guided by a fuzzy set of 27 rules that are usually stated as "if-then" statements in this editor. Fuzzy values are assigned to Final preference ($\tilde{y}_i$) by the grey-fuzzy analysis. Fuzzification processes use a triangle membership function (TMF) for each input, with subsets of fuzzy linguistic variables classified as small (S), medium (M), or large (L). Each segment of the GRC range, which goes from 0 to 1 is represented by one of these subsets. Finally, defuzzification module takes FIS's fuzzy output and turns it into a sharp numerical number. To convert fuzzy language variable into clean output, nine TMF were used as shown in Figure 3.

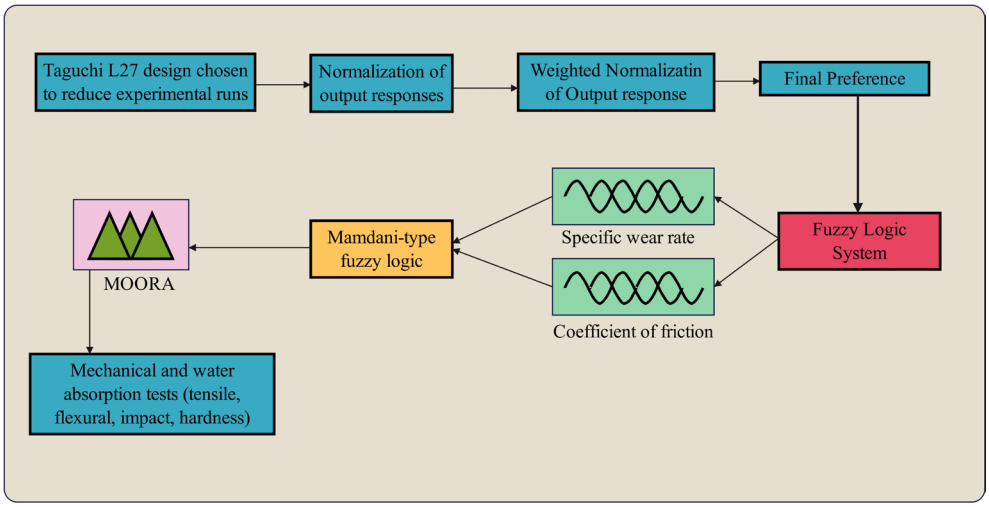

Fig. 2. Proposed grey–fuzzy logic method.

Figure 3 shows the nine fuzzy linguistic terms used to describe the outcomes of the defuzzification process, which are called MOORA Fuzzy Analysis (MFA). A membership function, denoted as t_1 represents specific wear rate and t_2, the coefficient of friction, respectively, is connected each of these linguistic phrases. Another way that Y, output response variable was represented is as MFA variable.

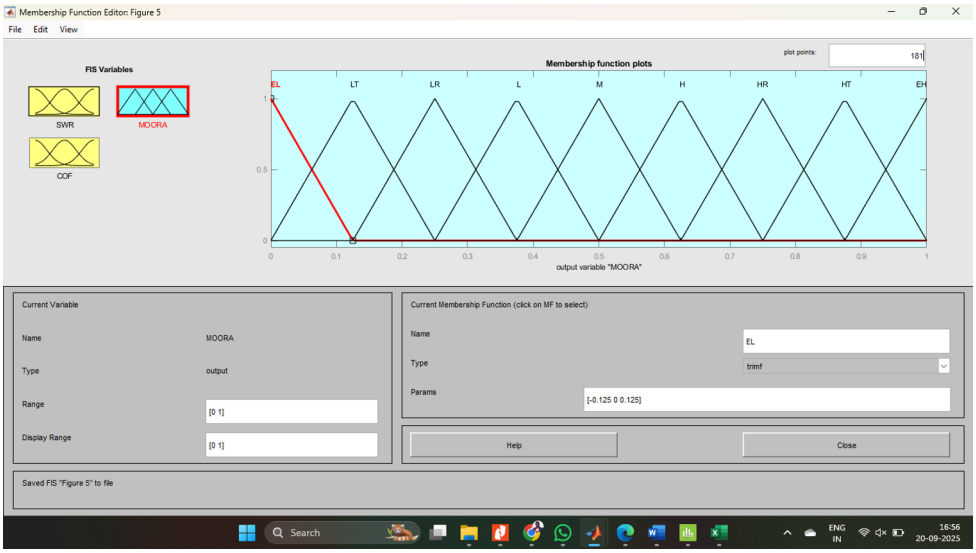

Fig. 3. Defuzzification of linguistic variables by Nine-TMF.

Two input variables, t_1 and t_2, and output Y, are described by a set of twenty-seven fuzzy rules that are based on the IF-THEN norm. Remain compliant with these rules.
Rule 1: if t_1 is A_1 and t_2 is B_1 then Y is C_1; else
Rule 2: if t_2 is A_2 and t_2 is B_2 then Y is C_2; else
Rule 3: if t_3 is A_3 and t_3 is B_3 then Y is C_3; else
……
Rule 27: if t_n is A_n and t_n is B_n then Y is C_n else.
By connecting sets of output fuzzy variables with pairs of input linguistic variables, these rules enhance fuzzy inference. Using this rule basis, the inference engine processes input fuzzy sets and generates output fuzzy set based on the results. The next step is to defuzzify the output, which gives a quantitative description of the system's output. Time variables t1, t2, and t3 are the independent variables. The membership functions, μAi and μBi, of the different fuzzy subsets, Ai and Bi, respectively, explain them. Based on these IF- THEN conditions, the total MFA (multi-response output) is computed by applying the max-min operation to subsets of linguistic variables along the TMF. The mathematical expression for this procedure is given by Eq. 14.

$$\mu C_0(Y_0) = \mathrm{Max}[\mathrm{Min}_u\{\mu\, A_1 t_1(t_1), \mu B_2 t_2(t_2) \ldots\ldots\ldots\ldots \mu Ct_n(t_n)\}] \quad (14)$$

The defuzzifier's job is to use Eq. 15 to transform the fuzzy inference output, which is denoted as μ_i, t_i into a numerical value that is not fuzzy. This result is in line with the MOORA Fuzzy Analysis (MFA)

$$y^y = \frac{\sum y\mu C_0(y_0)}{\sum \mu C_0(y_0)} \quad (15)$$

Keep in mind that the MOORA Fuzzy Approach (GFA) ideally achieves a lower GRG than the MFA value when comparing the two. After processing the fuzzy output, the fuzzy inference system (FIS) finds its centroid using the Centroid of Area (COA) technique.

2.7 Confirmation test

By running a confirmation test, we verified that the peak performance of particle natural hybrid composites could be accurately predicted by reducing the multi-response outputs. The confirmation test result was supported by the MFA value. To determine the MFA under perfect conditions, we utilized Eq. (16).

$$y_{\text{predicted}} = y^{y} + \sum_{i=1}^{n} y_{j-} y^{y} \quad (16)$$

The sum of the MFA values at the optimal point is represented by, y_{i}., the average MFA value is represented by, y_{y}, and the number of factor conditions is denoted by η.

3 Results and discussions

3.1 Multi response optimization using entropy and Moora

3.1.1 Entropy weighting technique

Based on the data in Table 2, L27 orthogonal array were created using the MINITAB 20 software. This presents the experimental data organized according to the Design of Experiments (DoE) methodology.

Table 2. Taguchi L27 orthogonal array design and experimental results.

S. No.	Input Parameter					Output Response	
	A: Gr/TiC (wt.%)	B: Rein forcement (wt.%)	C: Sliding distance	D: Sliding speed	E: Load	SWR	COF
1	1.5	15	450	0.6	6	5.062	0.401
2	1.5	15	450	1.2	12	5.336	0.476
3	1.5	15	450	1.8	18	6.003	0.652
4	1.5	25	900	1.2	18	5.088	0.543
5	1.5	25	900	1.8	6	5.16	0.666
6	1.5	25	900	0.6	12	5.345	0.748
7	1.5	35	1350	1.8	12	4.988	0.671
8	1.5	35	1350	0.6	18	5.094	0.807
9	1.5	35	1350	1.2	6	5.17	0.757
10	2.5	15	900	0.6	6	4.866	0.383
11	2.5	15	900	1.2	12	5.21	0.37
12	2.5	15	900	1.8	18	5.554	0.637
13	2.5	25	1350	1.2	18	5.027	0.553
14	2.5	25	1350	1.8	6	5.035	0.675
15	2.5	25	1350	0.6	12	5.144	0.707
16	2.5	35	450	1.8	12	4.934	0.722
17	2.5	35	450	0.6	18	4.995	0.676
18	2.5	35	450	1.2	6	5.117	0.688
19	3.5	15	1350	0.6	6	4.554	0.233
20	3.5	15	1350	1.2	12	4.898	0.266
21	3.5	15	1350	1.8	18	5.17	0.409
22	3.5	25	450	1.2	18	4.684	0.363
23	3.5	25	450	1.8	6	4.734	0.504
24	3.5	25	450	0.6	12	4.828	0.58

25	3.5	35	900	1.8	12	4.512	0.397
26	3.5	35	900	0.6	18	4.531	0.406
27	3.5	35	900	1.2	6	3.928	0.515

The decision matrix for the entropy weighting approach was normalized utilizing Equation (7). Based on Equations (8 - 10), the values for entropy measure (Ej), dispersion measure (Dj), and attribute weight (ωj) were calculated and shown in Table 3.

Table 3. Entropy method results.

	SWR	**COF**
Ej	0.956	0.943
Dj	0.10096	
Ωj	0.439	0.561

3.1.2 MOORA method

Making the selection matrix in Table 2 is the first step in the process. The results were adjusted for standard deviation using Equation 11. Table 4 displays the weights that are applied to the normalized data in real-time according to the relevance of the criteria. Table 4 shows the results of using the entropy approach to determine the weights of each criterion. The last step is to calculate the preference values using Equation 13. In conclusion, the materials were ranked based on the order of preference values, as shown in Table 4.

Table 4. MOORA optimization results.

S. No.	**Normalization**		**Weighted Normalization**		**Final Preference**	**Rank**
	WR	**COF**	**WR**	**COF**		
1	0.19434	0.13526	0.08536	0.07585	0.1612	20
2	0.20486	0.16056	0.08999	0.09003	0.1800	16
3	0.23047	0.21992	0.10123	0.12332	0.2246	4
4	0.19534	0.18316	0.0858	0.1027	0.1885	15
5	0.1981	0.22464	0.08702	0.12597	0.2130	9
6	0.20521	0.2523	0.09014	0.14148	0.2316	2
7	0.1915	0.22633	0.08412	0.12692	0.2110	12
8	0.19557	0.2722	0.0859	0.15264	0.2385	1
9	0.19849	0.25534	0.08719	0.14318	0.2304	3
10	0.18682	0.12919	0.08206	0.07244	0.1545	22
11	0.20002	0.1248	0.08786	0.06998	0.1578	21
12	0.21323	0.21486	0.09366	0.12048	0.2141	8
13	0.193	0.18653	0.08477	0.1046	0.1894	14
14	0.19331	0.22768	0.08491	0.12767	0.2126	10
15	0.19749	0.23847	0.08675	0.13372	0.2205	5
16	0.18943	0.24353	0.08321	0.13656	0.2198	6

17	0.19177	0.22802	0.08423	0.12786	0.2121	11
18	0.19645	0.23207	0.08629	0.13013	0.2164	7
19	0.17484	0.07859	0.0768	0.04407	0.1209	27
20	0.18805	0.08972	0.0826	0.05031	0.1329	26
21	0.19849	0.13796	0.08719	0.07736	0.1645	18
22	0.17983	0.12244	0.07899	0.06866	0.1476	25
23	0.18175	0.17	0.07983	0.09533	0.1752	17
24	0.18536	0.19564	0.08142	0.1097	0.1911	13
25	0.17323	0.13391	0.07609	0.07509	0.1512	24
26	0.17396	0.13695	0.07641	0.07679	0.1532	23
27	0.15081	0.17371	0.06624	0.09741	0.1636	19

The table 4. shows that the eigth experimental trial had the best performance out of all the combinations that were investigated, with a final performance value of 0.2385.

3.1.3 MOORA fuzzy analysis

All experiments were run in the fuzzy inference system environment of MATLAB R2020b to determine the MOORA Fuzzy Analysis (MFA) values. The particular wear rate (0.0872) and coefficient of friction (0.159) are shown by the final performance in Figure 4. Using the fuzzy rule base editor, 27 separate tests were conducted and their organized results are shown in Table 2.

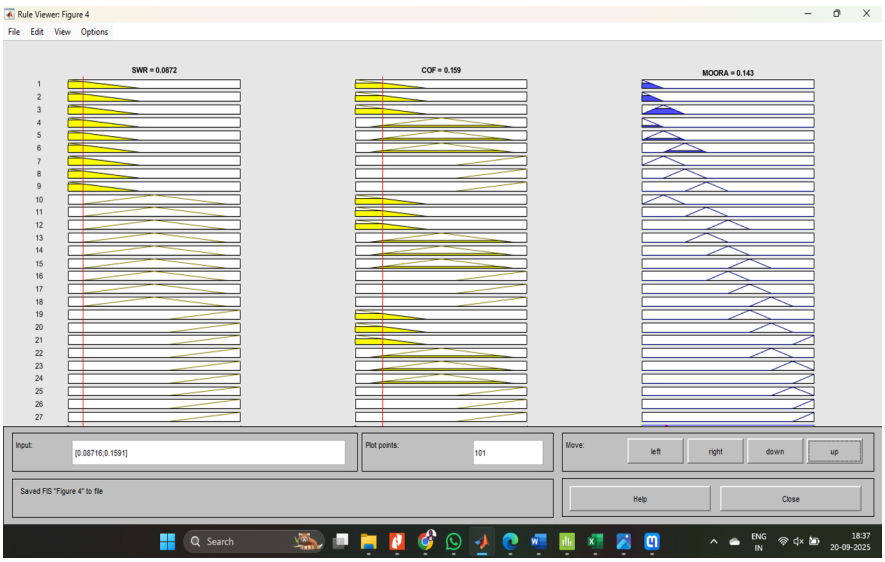

Fig. 4. Output response of MFA using fuzzy inference rules.

3.2 SEM analysis of worn surfaces

Under different wear and coefficient of friction conditions, SEM images of the wear morphology of particle-reinforced hybrid composites were examined (Figure 5(a) to Figure 5(c)) revealing the mechanisms of surface degradation at high magnification.

3.2.1 High wear with low CoF

The surface depicted in Figure 5a exhibits matrix cracking, indicative of abrasive wear. Localized brittle fracture of TiC particles is seen, accompanied by tiny grooves aligned with the sliding direction. These characteristics indicate inadequate tribofilm development under lower stress levels, when the combined effects of fiber reinforcing and ceramic filler are less efficacious. The particular wear rate in this scenario was 6.00×10^{-5} mm³/N·m, accompanied by a low coefficient of friction of 0.233, indicating less interfacial friction but increased surface damage due to inadequate protection.

3.2.2 High wear with high CoF

Under increased stress and sliding velocity, the abraded surface displays riverine patterns. The epoxy matrix exhibits significant distortion, resulting in less adhesion between the fibers and the matrix.

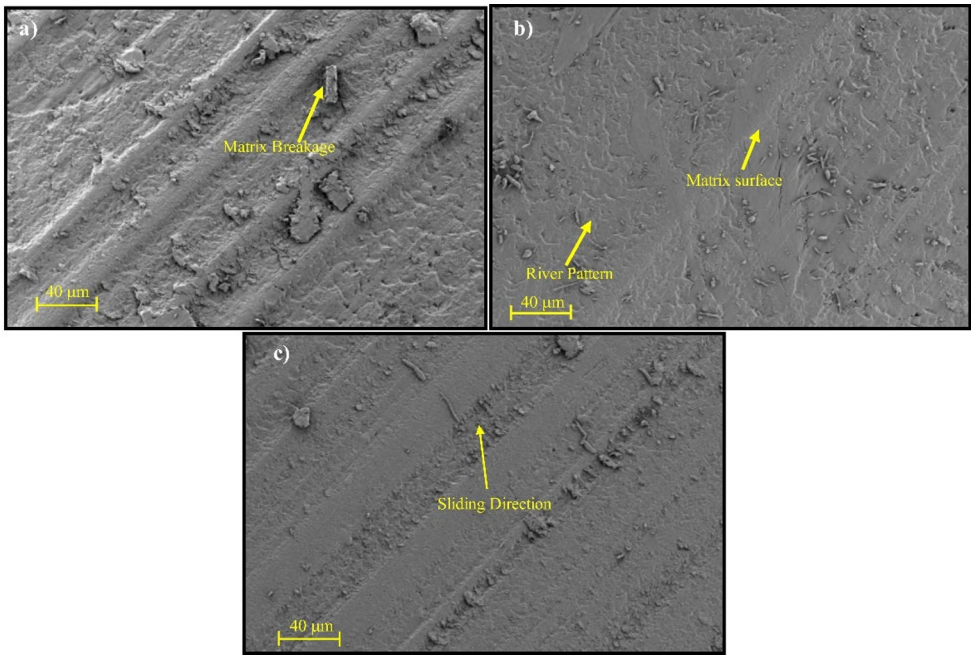

Fig. 5. (a-c) SEM images of worn surfaces at different TiC content, fiber reinforcement, and tribological conditions.

The elevated interfacial shear stress constrains the protective efficacy of TiC fillers and inhibits the development of a continuous tribofilm.

This leads to a 20.3% escalation in wear rate and a 62.5% augmentation in coefficient of friction (COF) relative to the optimal condition, underscoring that severe pressures induce a shift from mild abrasive wear to a hybrid abrasive-adhesive wear mechanism. Bamboo fiber-reinforced polyester composites toughened with silane-treated lignin from grape stalks were developed, while the 4.0 vol% lignin composite exhibited the best wear resistance with a low specific wear rate of 0.007 mm^3/Nm as observed in previous studies [11]. Under optimal tribological circumstances, the worn surface exhibits a smooth shape characterized by continuous sliding grooves. The uniform distribution of TiC particles occupies microcracks and improves adhesion at the fiber-matrix interface, facilitating the development of a stable, adherent tribofilm. This protective layer minimizes material loss and absorbs frictional energy more efficiently.

3.3 Moisture uptake and retained mechanical properties

Composites reinforced with natural fibers are more likely to absorb moisture in wet or watery conditions because of their intrin TiC hydrophilic nature, caused by the presence of hydroxyl groups in the cellulose molecule. In light of its possible use in both dry and wet settings, this study set out to maximize the wear resistance of a hybrid composite material composed of bamboo and PALF particles reinforced with titanium carbide (TiC). For this reason, we measured the composite's tensile strength, flexural strength, and impact resistance both before and after it was wetted.

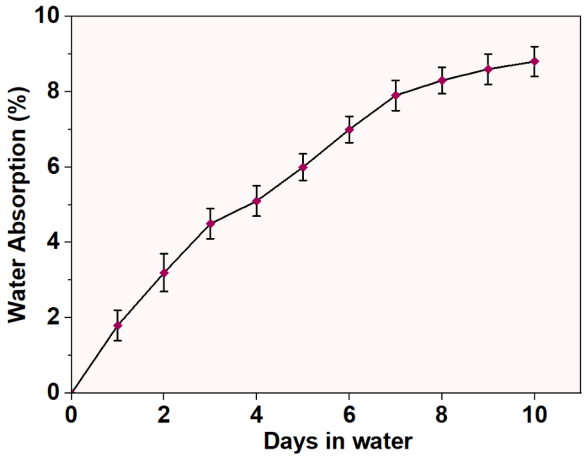

Fig. 6. Hydrophilic behaviour of 1 wt.% TiC reinforced Bamboo/PALF hybrid composite.

Microcracks developed at matrix-fiber interface because of water absorption-induced fiber swelling, which was resulted by differential expansion and matrix debonding. Optimal composite structure water uptake behavior is illustrated in Figure 6. Using Eq. (4), we determined the water absorption percentage and then plotted it against immersion time. The results showed that water uptake increased with time, reaching the highest of 8.8% for best-designed hybrid system—a significant decrease from the generally acknowledged 10% stability limit at polymer composites. A minimum of 1.8% absorption was noted following 48 hours of immersion. The optimized system showed much lower water uptake compared to a control bamboo/PALF composite with a 30 wt.% loading of bamboo fibers, with a water absorption value of 8.8%. Water absorption rates of about 1.8% have been observed in PALF fiber reinforced polyethylene composites with a fiber loading of 30 wt.%.

By highlighting the increased hydrophilicity of bamboo fibers compared to PALF, this difference supports the idea that natural fiber composites can be effectively countered by hybridizing with PALF and adding TiC fillers (Figure 5(a) to Figure 5(c)). There was a consistent pattern of fast water uptake at the outset, followed by a slowing of the rate of absorption, and finally saturation as the immersion time increased in all of these hybrid composites. In addition, both dry and wet samples of the particle hybrid composites were tested for mechanical properties, such as tensile, flexural, and impact. As demonstrated in Figure 7(a) and Figure 7(b), the mechanical characteristics declined by 10% during the water absorption test, according to the experimental data. This reduction occurred because the interphase area swelled and spiked after being attacked by water molecules for an extended length of time, which in turn made it weaker. Swelling fibers alter their diameters as well, leading to the appearance of microcracks on the matrix surface. Immersion periods that were longer enabled bigger water molecules to cross the composite's interphase and separate the matrix from the fibers.

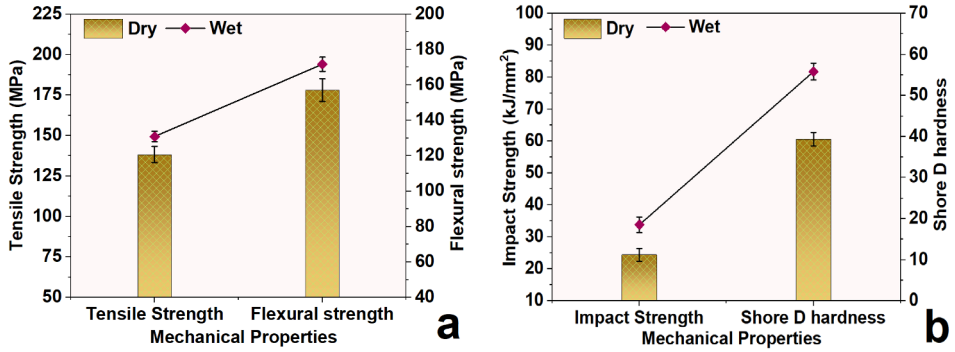

Fig. 7. Effect of 1 wt% TiC Addition on Mechanical properties of Bamboo/PALF (30 wt%) hybrid composite (a) Tensile strength & flexural strength, and (b) Impact strength & shore d hardness.

A composite's mechanical characteristics may be heavily influenced by the degree to which its fibers and matrix adhere to one another. The mechanical integrity of the composite kept deteriorating as the immersion period increased. The TS of particulate hybrid composite was 138.2 MPa, which is significantly higher than the 39 MPa demonstrated by most composites with 30wt% long bamboo fiber. The effectiveness of hybridization and filler addition is highlighted by these changes. NaOH-treated bamboo fibers were incorporated into GFRP composites with 1% TiO_2 filler. At 0.5% fiber content, the composites achieved maximum tensile (155 MPa), showing strong potential for structural and aerospace use [12]. The increased impact resistance and hardness generated by swelling could be due to microcracks on the surface, debonding of the fiber and matrix, and capillary cracks. Water molecules constantly attack the interphase. Research suggests that combining bamboo and PALF can enhance the composite's strength and water resistance, while silica filler provides superior resistance to wear. Based on the findings, a composite material made of 30 wt.% bamboo (61.38 MPa) is stronger than a pure PALF composite (49.8 MPa), and a composite material made of particulate hybrid random (138.2 MPa) has a beneficial hybridization effect. The S9 laminate showed maximum strength flexural 47.55 MPa with SEM confirming fracture behavior, and the composites were suggested for tabletops, desks, and boards as reported by [13]. In addition, the composite's tribological behavior is determined by its mechanical properties, which in turn determine the material's resistance to deformation. Raising the hardness typically slows the wear rate since less material is removed. A particulate hybrid random composite has a hardness of 60.6 MPa, whereas a pure random

PALF composite has a hardness of 53.7 MPa and a random bamboo composite has a hardness of 58.7 MPa.

Brake pad composites using bamboo fiber and dried clove leaves as reinforcements in polyester/MEKP resin were investigated. Smaller particle size and higher bamboo ratios improved hardness (24 N/cm²), and enhanced wear and friction properties, presenting a sustainable asbestos-free alternative [14]. Ploughing resistance and micro cutting, frictional behavior and surface degradation mitigation stabilization are all enhanced by the addition of 1 wt% TiC. Tribological durability was also improved due to decreased microcrack propagation and delamination brought about by increased impact resistance [15]. A pure random bamboo composite (23.3 kJ/mm^2) and a particulate hybrid random composite (27 kJ/mm^2) both offer strength, while a random PALF composite (30 wt.%) offers even more. Kevlar–PALF woven epoxy hybrids with different weaving patterns were examined. Basket-type composites showed superior impact (16.3 kJ/m²), indicating their suitability for automotive interior applications as observed by authors.

4 Conclusions

The effective method for studying the tribological characteristics of hybrid composites is MOORA-fuzzy multi-response modeling and optimization. An effective, methodical, and adaptable approach to optimizing for numerous answers is provided by this method. It was found that 1.5 wt.% TiC, 35 wt.% reinforcement, 1350m of sliding distance, 1.8mm/s of sliding speed, and 12N of load for safer operating circumstances were the best parameters to use when making hybrid composites with excellent tribological properties.

- On the other hand, when the TiC nanofiller content was too high, the particles clumped together, leading to rough tribo film and significant wear when subjected to strong sliding.
- The defuzzified output variable from the experimental trials was quite near to the reference line, as shown by the residual plot. Afterwards, the best set of parameters determined by the MOORA-fuzzy method was subjected to additional testing for mechanical capabilities after exposure and moisture absorption. A 8.8% reduction in water diffusivity and an increase in interfacial degradation were the results of a water absorption test showed how fiber-filler hybridization greatly improved moisture. When comparing wear resistance and mechanical strength, the optimal combination was 1.5wt% TiC with 35wt% fiber reinforcement. These results highlight the importance of optimal tribo-mechanical performance of bamboo/PALF-TiC hybrid composites, which is greatly improved by using an adequate TMF and fine-tuning the fuzzifiers.
- Images captured by scanning electron microscopy (SEM) of specimens that had already begun to wear down revealed the various wear mechanisms at work.
- In light-duty applications moderate wear resistance and low friction were required, such as sealing, cages, appliance sliders and bearings interfaces the resulting bamboo/PALF-TiC filled composite can be used for development and design under mild load conditions.

References

1. M. Vinoth Kumar, M. Kannaiyan, Development and characterization of ecofriendly polyester composites using bamboo fiber and cassava sheath biosilica. Biomass Conv. Bioref. 15, 20893 (2025). https://doi.org/10.1007/s13399-025-06644-z
2. P. S. Kumar, S. Prabagaran, S. R. Kandavalli, S. Rajeshkannan, Analysis of Sea Urchin Spike Chitin and Basalt Bamboo Fiber-Epoxy Composite for Environmental Sustainability. Waste and Biomass Valorization. 16, 1805 (2025). https://doi.org/10.1007/s12649-024-02728-5
3. Ajithram Arivendan, Sumesh KR, Xiaoqi Chen, Yuan-Fang Zhang, Wenhua Gao, Firda Aulya Syamani, Winowlin Jappes Jebas Thangiah, Combining the pineapple leaf fibre (PALF) and industrial ramie fibre to the epoxy matrix for high-strength light weight medium-density fibreboards. Biomass Conv. Bioref. 15, 4717 (2025). https://doi.org/10.1007/s13399-023-05243-0
4. G. Velmurugan, V. Siva Shankar, M. Kalil Rahiman, D. Elil Raja, M. Nagaraj, T. Nagalakshmi T, Experimental Investigation of High Filler Loading of SiO2 on the Mechanical and Dynamic Mechanical Analysis of Natural PALF fibre-Based Hybrid Composite. 15, 5587 (2023). https://doi.org/10.1007/s12633-023-02464-w
5. P. Thangavel, S. Vignesh, R. Sureshkumar, A. Gowrishankar, R. Girimurugan, Study on mechanical properties of polylactic acid matrix added with fly ash and tamarind kernel powder micro fillers. NanoWorld J. 9, S626 (2023).
6. K. Muralishwara, L. Fernandes, R. Kalkura, S. Bangera, Effect of Surface Modified Montmorillonite Nanoclay on Tensile and Flexural Properties of Pineapple Leaf Fiber Reinforced Epoxy Composite. Materials Research. 26, (2023). https://doi.org/10.1590/1980-5373-MR-2022-0437
7. Mohit Hemanth, Sanjay Mavinkere Rangappa, Suchart Siengchin, Ruban Ramalingam, Hadi M. Marwani, Anish Khan, Abdullah M. Asiri, Physico-mechanical, and thermal properties of sisal/hemp/Kevlar fibers, fly ash and Titanium Carbide nanoparticles reinforced bioepoxy composites. Polymer Composites. 44, 7117 (2023). https://doi.org/10.1002/pc.27622
8. A. Moorthy, K. Kanagaraj, M. Palanisamy, G. Ramasamy, Investigation of synthetic and natural cork fiber laminate polymer composite bending characteristics. Matéria (Rio de Janeiro). 29, e20240489 (2024). https://doi.org/10.1590/1517-7076-RMAT-2024-0489
9. W. Lei, S. Wang, Y. Xia, Y. Yang, Y. Zhang, W. Yu, Novel strategy for preparing high-performance bamboo-fiber-reinforced composite by designing bonding interface. Industrial Crops and Products. 233, 121388 (2025). https://doi.org/10.1016/j.indcrop.2025.121388
10. S. Fan, B. Li, Z. Ying, Z. Li, X. Gao, Synergistic enhancement of peroxyformic acid-refined long bamboo fibers via aqueous epoxy resin reinforcement for superior mechanical properties. Construction and Building Materials. 493, 143251 (2025). https://doi.org/10.1016/j.conbuildmat.2025.143251
11. H. Alshahrani, V. R. Arun Prakash, Mechanical, thermal, viscoelastic and hydrophobicity behavior of complex grape stalk lignin and bamboo fiber reinforced polyester composite. International Journal of Biological Macromolecules. 223, 851 (2022. https://doi.org/10.1016/j.ijbiomac.2022.10.272

12. S. Prashanth, R. Pongen, Y. K. Verma, S. Kumar, Enhancing GFRP composites with bamboo fiber and TiO2: a study on mechanical and tribological properties. Journal of Adhesion Science and Technology. 39, 1793 (2025). https://doi.org/10.1080/01694243.2025.2470258
13. V. Vinoth, S. Sathiyamurthy, N. Ananthi, P. Devi, Studies on Mechanical, Morphological, and Water Absorption Properties of Agro Residues Reinforced Polyester Hybrid Composites. Iranian Journal of Chemistry and Chemical Engineering 43, 2375 (2024). https://doi.org/10.30492/ijcce.2024.2014563.6285
14. R. Saravanan, R. Anand, C. Boopathi, L. G. Babu, A. Yasminebegum, G. Ravivarman, R. Girimurugan, Mechanical Properties of Polyethylene/Hemp/Lignin Hybridized Composites. International Journal of Vehicle Structures & Systems. 16, 738 (2024). https://doi.org/10.4273/ijvss.16.5.17
15. S. Jeyaguru, S. M. K. Thiagamani, H. Pulikkalparambil, S. Siengchin, S. Krishnasamy, A. G. Rajkumar, S. M. Rangappa, Effects of different weaving patterns on thermomechanical and dynamic mechanical properties of Kevlar/pineapple leaf fiber hybrid composites. Polymer composites. 43, 4979 (2022). https://doi.org/10.1002/pc.26764